Table 1 Structural control with velocity feedback, $\ddot{x} + C\dot{x} + \Lambda x = Bu$, $u = -K_v B_v^T \dot{x}$

	c/nc[a]	Condition	s/u[b]
1	c	$\Lambda > 0, K_v > 0$	s
2	$B = B_v$	$\Lambda < 0, K_v > 0$	u
3		$\Lambda > 0$, $C + 1/2(BK_vB_v^T + B_vK_v^TB^T) > 0$	s
4	nc	$\Lambda > 0$, $C + 1/2(BK_vB_v^T + B_vK_v^TB^T) < 0$	u
5		$\Lambda > 0, B^T = AB_v^T$, $K_v = LL^TA + T, T = -T^T$	s
6		$\Lambda > 0, B\, R^{n\times 1}$, $B = [b_i], B_v = [b_{vi}], b_i\, b_{vi} > 0$	s
7		$\Lambda < 0$, $C + 1/2(BK_vB_v^T + B_vK_v^TB^T) < 0$	u
8	$B \neq B_v$	$\Lambda < 0, C = 0, (4\Lambda - GG) > 0$ $G = 1/2(BK_vB_v^T + B_vK_v^TB^T)$	s
9		$\Lambda < 0, C = 0, (4\Lambda - GG) < 0$ $G = 1/2(BK_vB_v^T + B_vK_v^TB^T)$	u

[a]c/nc: colocated/noncolocated.
[b]s/u: stable/unstable

criteria guarantee a stable closed-loop system with infinite gain margin. One can achieve simultaneously both the damping argumentation and the energy transfer between vibration modes. Only the noncolocated feedback has the potential of stabilizing an unstable system. These constructive designs have not been reported as yet. The stability criteria are summarized in Table 1.

Conclusions

1) A stability robustness criterion of second-order structure systems with noncolocated velocity feedback is developed. Conditions are derived in terms of the structure inertia, damping, and stiffness matrices and the feedback control gain that guarantee the closed-loop stability.

2) Colocated velocity feedback on nongyroscopic structure systems is always constructive because of positive damping argumentation. The closed-loop system is asymptotically stable with infinite gain margin. Similarly, the closed-loop system with noncolocated feedback is also stable, provided that the symmetric part of the generalized damping matrix is positive definite. Stability robustness criteria are listed in Eqs. (6) and (7). One can achieve simultaneously both the damping argumentation and the energy transfer between vibration modes.

3) A gyroscopic structure system, e.g., a stable spinning top, can remain stable at some negative stiffness state, $\Lambda < 0$, but the application of colocated velocity feedback leads to an unstable system. This is one unique case where colocated velocity feedback, contrary to common belief, destabilizes an otherwise stable system. Similarly, an unstable system $\Lambda < 0$ can never be stabilized by colocated velocity feedback; a noncolocated pair is required for stabilization.

4) It is important to know that all the previous analysis shown, and hence the stability robustness criteria, are developed in the absence of actuator and sensor dynamics. Goh and Caughey[13] have indicated that second-order actuator dynamics can affect the stability robustness, provided that the actuator mass, damping, and stiffness properties are known. Spanos[14] also showed that sensor dynamics could limit the stability robustness. Further work on developing the stability robustness criteria for systems with both sensor and actuator dynamics is necessary.

References

[1]Schafer, B. E., and Holzach, H., "Experimental Research on Flexible Beam Modal Control," *Journal of Guidance, Control, and Dynamics*, Vol. 8, No. 5, 1985, pp. 597–604.

[2]Parks, T. R., and Pak, H. A., *Journal of Dynamic Systems, Measurement, and Control*, Vol. 113, 1991, pp. 409–418.

[3]Balas, M. J., "Feedback Control of Flexible Structure," *IEEE Transactions on Automatic Control*, Vol. AC-23, No. 4, Aug. 1978, pp. 673–679.

[4]Thomas, H. L., and Schmit, L. A., "Control-Augmented Structural Synthesis with Dynamic Stability Constraints," *AIAA Journal*, Vol. 29, No. 4, 1991, pp. 619–626.

[5]Cannon, R. H., and Rosenthal, D. E., "Experiments in Control of Flexible Structure with Noncolocated Sensors and Actuators," *Journal of Guidance, Control, and Dynamics*, Vol. 7, No. 5, 1984, pp. 546–553.

[6]Kliem, W., and Pommer, C., "On the Stability of Linear Nonconservative Systems," *Journal of Applied Mathematics*, Vol. 43, No. 4, Jan. 1986, pp. 456–461.

[7]Ahmadian, M., and Inman, D. J., "Some Stability Results for General Linear Lumped-Parameter Dynamic Systems," *Journal of Applied Mechanics*, Vol. 53, March 1986, pp. 10–14.

[8]Piche, R., "On the Symmetrizability of Structure Control Systems with Noncolocated Sensors and Actuators," *Journal of Dynamic Systems, Measurement, and Control*, Vol. 112, June 1990, pp. 249–252.

[9]Zhang, Q., and Shelly, S., "Active Damping Design of Flexible Structures Based on SISO and SIMO Noncolocated Sensor-Actuator Velocity Feedback," *Journal of Dynamic Systems, Measurement, and Control*, Vol. 113, June 1991, pp. 259–266.

[10]Yang, S. M., and Mote, C. D., "Stability of Nonconservative Linear Discrete Gyroscopic Systems," *Journal of Sound and Vibration*, Vol. 140, No. 2, 1991, pp. 453–464.

[11]Martin, G. D., and Bryson, A. E., "Attitude Control of a Flexible Spacecraft," *Journal of Guidance, Control, and Dynamics*, Vol. 3, No. 1, 1980, pp. 37-41.

[12]Williams, T., "Transmission-zero Bounds for Large Space Structure with Application," *Journal of Guidance, Control, and Dynamics*, Vol. 12, No. 1, 1989, pp. 33–38.

[13]Goh, C. J., and Caughey, T. K., "On the Stability Problem Caused by Finite Actuator Dynamics in the Colocated Control of Large Space Structures," *International Journal of Control*, Vol. 41, No. 3, 1985, pp. 787–802.

[14]Spanos, J. T., "Control Structure Interaction in Precision Point Servo Loops," *Journal of Guidance, Control, and Dynamics*, Vol. 12, No. 2, 1989, pp. 256–263.

Nonlinear Response of Asymmetrically Laminated Plates in Cylindrical Bending

Erasmo Carrera*
DIAS-Politecnico di Torino, Torino 10129, Italy

I. Introduction

THE increasing use of high performance materials has intensified the demand for the development of tools to trace the response of laminated structures made by differently oriented laminas. Composite plates asymmetrically laminated (with respect to the middle surface of the laminate) are seldom used in structures, mainly because of the difficulty in controlling their configuration after curing. In reality, however, an asymmetric laminate may result from delamination, from surface damage in symmetric laminates, and from some geometrical imperfections in the thickness and/or in the orientation of each lamina. Since the pioneering studies made by Ambartsumyan[1] and Stavsky and Reissner[2] revealed the bending-stretching coupling effect in laminate composite plates, a considerable amount of work based on several theories and approximate methods of solution has been done on the nonlinear analysis of such plates. In fact, for the symmetric laminates, linear laminate plate theory is quite adequate if the transverse deflection is small compared with the plate thickness. But in an asymmetrically laminated plate, lateral deflection, i.e., plate bending, may be involved immediately when the load is applied, even though only in-plane loading exists. This early bending-extension coupling causes linear lamination theory to yield large errors in analyzing asymmetric laminates. As a consequence, their response should be computed

Received June 9, 1992; revision received Dec. 5, 1992; accepted for publication Dec. 5, 1992.

*Research Engineer, Corso Duca degli Abruzzi 24. Member AIAA.

by employing models on the basis of the nonlinear theories. For a compendium of the work made in the literature, see Chia,[3] Leissa,[4] Sun and Chin,[5,6] Barbero and Reddy,[7] Carrera,[8] and the recent book of Palazotto and Dennis.[9]

As is well known, the computational costs of nonlinear analyses are very high, mainly because a nonlinear system of equations must be solved iteratively at each load step. To handle the problem in a rather simple manner, Sun and Chin[5] have recently presented a closed-form solution concerning the large deflection analysis in cylindrical bending of asymmetrically laminated plates. The bending is given by in-plane axial and transverse loads. The von Kármán nonlinear theory in connection with classical lamination theory (CLT) is employed. The results are compared to finite element method (FEM) analysis. For the in-plane loading cases, the authors have restricted the numerical investigations to the tension case, finding a very good agreement with the FEM results. The results are compared to the linear analytical solution. In a subsequent paper,[6] the same authors have presented the extension to the in-plane compression loading case of their closed-form solution. In Ref. 6 the results are not compared to the FEM solutions. More recently, Chen and Shu[10] have presented the extension of the Sun and Chin theory to shear deformable plates.

The research work in this Note starts with a discussion of Sun and Chin's works. Concerning the in-plane loading case, Sun and Chin's nonlinear theory leads to some questionable results which are typical of linearized solutions. That throws some doubt on its correctness as a tool to trace the nonlinear response of asymmetrically laminated plates (see Sec. II). For comparison purposes a nonlinear finite element plate model is employed. Further, for the axial compression in-plane loading case, the FEM analysis will show a rather new result: the possibility of finding a limit point in the load-displacement path, i.e., snap-through type of phenomena. A one-degree-of-freedom model will offer a very simple interpretation of each of the treated problems. The three models are presented here in different sections.

II. Analytical Model

Let us consider an asymmetric cross-ply laminate subjected to a uniform in-plane loading. For a cylindrical bending type problem we assume that the governing equations are independent of the longitudinal direction (y axis). The equilibrium equations based on the von Kármán large deflection theory in conjunction with the CLT assumptions are given in Refs. 5 and 6. They are

$$N_{x,x} = 0; \qquad M_{x,xx} + N_x w_{,xx} = 0 \tag{1}$$

where M_x and N_x are the classical stress resultants,[3] w is the transverse deflection, and the comma denotes a partial derivative with respect to the longitudinal direction (x axis). Given some latitude, Eqs. (1) and related boundary conditions could also be derived from those quoted in Ref. 11. A closed-form solution of Eqs. (1) with appropriate boundary conditions has been presented in Refs. 5 and 6. We refer to these works for additional information. A brief description related to the in-plane loading case, which is useful for our purposes, is included in the following text. From the first of Eqs. (1), we conclude that the stress resultant N_x has the same value N_x^0 at each point of the plate. Consequently, Eqs. (1) become

$$N_x = N_x^0; \qquad M_{x,xx} + N_x^0 w_{,xx} = 0 \tag{2}$$

The nonlinearities in M_{xx} can be eliminated by employing the constitutive equations[3]

$$N_x = A_{11}(u_{,x} + \tfrac{1}{2} w_{,x}^2) - B_{11} w_{,xx}$$

$$M_x = B_{11}(u_{,x} + \tfrac{1}{2} w_{,x}^2) - D_{11} w_{,xx} \tag{3}$$

where A_{11}, B_{11}, and D_{11} are the well-known membrane, coupling (membrane bending), and bending plate stiffnesses, respectively; u denotes the displacements along the x axis. Taking into account the first of Eqs. (2), Eqs. (3) lead to

$$M_x = \frac{B_{11}}{A_{11}} N_x^0 + \left(\frac{B_{11}^2}{A_{11}} - D_{11}\right) w_{,xx} \tag{4}$$

which is linear. Thus, the governing equation remains

$$w_{,xxxx} - k^2 w_{,xx} = 0 \tag{5}$$

where $k^2 = N_x^0/[D_1 - (B_{11}^2/A_{11})]$. Equation (5) consists of a linear differential equation with constant coefficients. Consider an asymmetric cross-ply laminate subjected to a uniform in-plane load N_x^0 along the two simply supported straight edges: $w = 0$, $M_x = 0$ at $x = \pm a$ ($2a$ is the plate length). The other two edges are obviously free. By imposing these boundary conditions, the solutions of Eq. (5) hold

$$N_x^0 > 0: \qquad w(x) = \frac{B_{11}}{A_{11}}\left[\frac{\cosh(kx)}{\cosh(ka)} - 1\right]$$

$$N_x^0 < 0: \qquad w(x) = \frac{B_{11}}{A_{11}}\left[\frac{\cos(kx)}{\cos(ka)} - 1\right] \tag{6}$$

where $N_x^0 > 0$ and $N_x^0 < 0$ are tension and compression, respectively. Equations (6) give a nonlinear relation between the applied load N_x^0 and the normal deflection w. That happens because the coefficient k^2 is N_x^0 dependent. The maximum deflection at the center of the plates holds

$$N_x^0 > 0: \qquad W_c = \frac{B_{11}}{A_{11}}\left[\frac{1}{\cosh(ka)} - 1\right]$$

$$N_x^0 < 0: \qquad W_c = \frac{B_{11}}{A_{11}}\left[\frac{1}{\cos(ka)} - 1\right] \tag{7}$$

In the N_x^0-W_c plane, the tension case gives the vertical asymptote $W_{max} = -(B_{11}/A_{11})$ as $N_x^0 \to \infty$, whereas the compression case gives the horizontal asymptote $N_{max} = -(\pi/2a)^2 [D_{11} - (B_{11}^2/A_{11})]$ as $W_c \to \infty$. Consider the lamina properties and plate geometry given in Ref. 5: $E_l = 20$ msi (0.1379 MPa), $E_t = 1.4$ msi (0.0097 MPa), $G_{lt} = G_{tt} = 0.7$ msi (0.00048

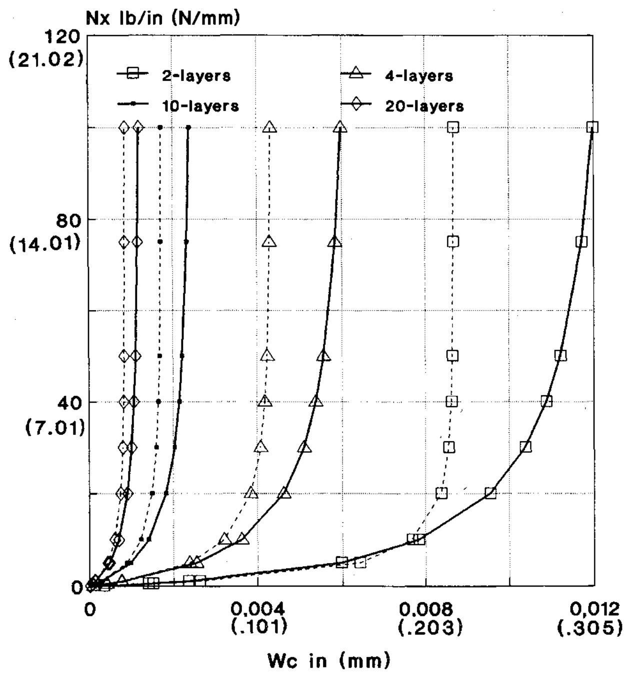

Fig. 1 **Comparison between the analytical and FEM models, tension case: load deflection curves for several numbers of layers; — FEM model, - - analytical model.**

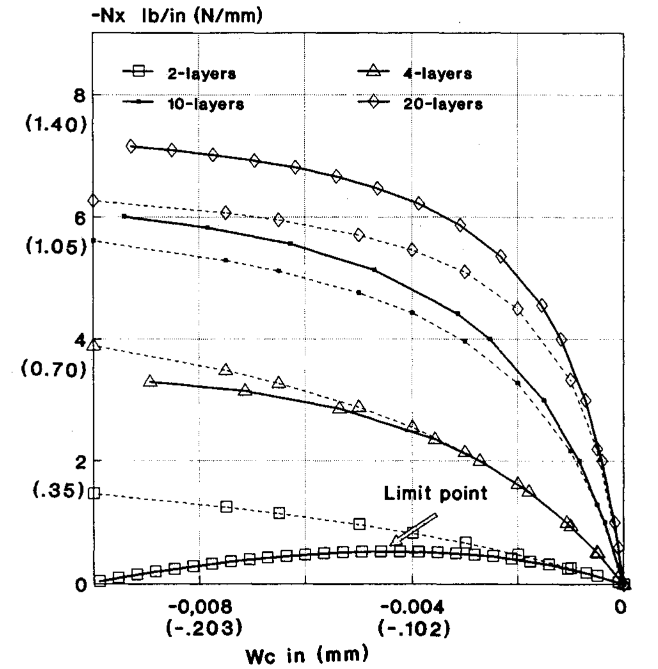

Fig. 2 Comparison between the analytical and FEM models, compression case: load deflection curves for several numbers of layers; — FEM model, - - analytical model.

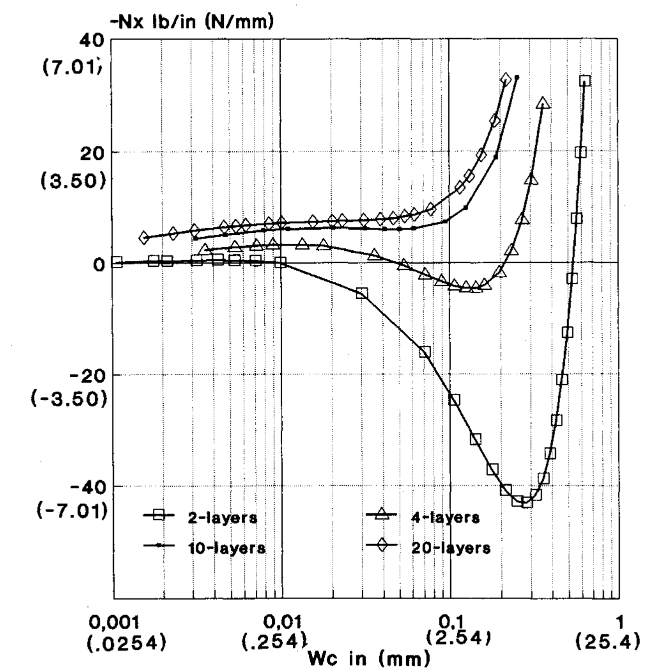

Fig. 3 FEM model, compression case: load deflection curves for several numbers of layers in logarithmic scale.

MPa), $\nu_{lt} = 0.3$; length $2a = 9$ in. (228.6 mm), width $2b = 1.5$ in. (3.81 mm), and thickness $t = 0.04$ in. (1.016 mm). For comparison purposes we refer to the English units as in Ref. 5 and 6; with the exception of Table 1, the metric values will be written in brackets. Four L values are investigated (L denotes the number of layers). Figures 1 and 2 show the response of Eqs. (7) in the N_x^0-W_c plane as well as the FEM results which we will discuss in Sec. III. By the compression case we conclude that the plates cannot withstand loads greater than those given by $N_{\max}$. This result throws some doubt on the validity of the Sun and Chin model as a tool to trace the nonlinear response of cylindrical bending of asymmetrically laminated plates. In fact, the asymptote $N_{\max}$ of Fig. 2 is a typical result of a linearized buckling problem as described in Ref. 6 as well as what we will show subsequently. Furthermore, the Fig. 2 results seem quite different from those typically found by other authors; see, for example, Refs. 7 and 8.

In the end of this section, we want to show the linearized nature of the analytical model proposed in Refs. 5 and 6. To do this, Eqs. (4) will be obtained in a different manner with respect to that given earlier. In addition, we will remark that the load value $N_{\max}^0$ coincides to the lowest eigenvalue of the linearized stability equations.

Taking Eqs. (1) and (2) as correct, we linearize Eqs. (3)

$$N_x \sim N_x^l = A_{11}u_{,x} - B_{11}w_{,xx}$$

$$M_x \sim M_x^l = B_{11}u_{,x} - D_{11}w_{,xx} \tag{8}$$

By the use of these equations instead of Eqs. (3), we obtain the same Eqs. (4) and (5). The algebraic manipulations are exactly the same as those in Ref. 5. It is now explicitly clear that Eqs. (4) and (5) are also valid for the assumptions of Eqs. (8). As a consequence, the unique nonlinearity comes from the term $N_x^0 w_{xx}$. In fact, this remains a very incorrect conclusion; as we have stated in the Introduction, the main characteristic of asymetrically laminated plates consists of having large deflections w even if the applied level of loads considered is low, and they cannot be neglected.

At this point we can note the hypotheses on which the Sun and Chin solution is based: 1) the stress resultant N_x is the constant in the plate and 2) the nonlinear terms in Eqs. (8) are neglected. As is well known, these hypotheses are the conditions under which the buckling loads of symmetrically laminated plates can be computed as a classical problem of Euler stability[12] (the conditions under which assumptions 1 and 2 are verified for asymmetrically laminated plates are discussed in Ref. 4). Because these assumptions are based on Eqs. (5), then the asymptote $N_{\max}^0$ must be found as the first eigenvalue of the linearized stability equations. In fact, by assuming the shape functions (see Refs. 6, 11, and 12), $u(x) = A^u \sin(m\pi x/2a)$ and $w(x) = A^w \cos(m\pi x/2a)$, which satisfy the simply supported boundary conditions (m denotes the half-wave number in the x direction, whereas A^u and A^w are the amplitudes of u and w, respectively), then the following classical value of the buckling load arises: $N_{cr} = -(m\pi/2a)^2[D_{11} - (B_{11}^2/A_{11})]$. The lowest value $m = 1$ corresponds to the values of $N_{\max}$.

By examination of the different order of magnitude of N_x^0 in Figs. 1 and 2, we can foresee that the tension case should be more accurate than the compression case. In fact, the results in Fig. 1 show that in the neighborhood of the asymptote, the plates become very stiff, and since W_c is small with respect to N_x^0, the effect of the approximations Eqs. (8) cannot be all that dramatic. Further, in these loading cases, the most important nonlinear terms $N_x^0 w_{,xx}$ have been taken into account. The trend reverses in the axial compression case. We will come back to these questions to confirm them when we compare the analytical model to the FEM results. Concluding this section we remark that the derivations of Eqs. (4) and (5) made in Ref.

Table 1 Comparison between linear and nonlinear results of the analytical and FEM analyses on W_c, in.

		Analytical model		FEM model	
N_x^0, lb/in.	Layers	Linear	Nonlinear	Linear	Nonlinear
0.1	2	3.513E-4	3.398E-4	3.536E-4	3.334E-4
0.1	10	3.130E-5	3.084E-5	3.136E-5	3.098E-5
10	2	3.513E-2	7.671E-3	3.536E-2	7.832E-2
10	10	3.130E-3	1.227E-3	3.136E-3	1.414E-2
−0.1	2	−3.513E-4	−3.636E-4	−3.536E-4	−3.781E-4
−0.1	10	−3.130E-5	−3.178E-5	−3.136E-5	−3.175E-5
−3	2	−1.054E-2	−7.049E-1	−1.061E-2	[a]
−3	10	−9.390E-3	−1.694E-3	−9.408E-3	−1.504E-3

[a]Failure of the load control method.

5 are mathematically unexceptional, but in deriving them some nonlinear terms are tragically lost. This does not happen in the FEM model, where the external loads are directly imposed in the equilibrium equations.

III. Finite Element Method Model

To compare the results of the analytical model and to show its inadequacy in predicting the nonlinear response of asymmetrically laminated plates, this section presents a nonlinear FEM model of the problem considered in Sec. II. The results in Refs. 5 and 6 will not be confirmed and a different level of accuracy of the analytical model, in tension and compression, will be established. Furthermore, by trying several values of B_{11} a quite new result concerning the nonlinear response of axially compressed long plates will be found: the possibility of a snap-through type of phenomena.

An eight-node Mindlin type isoparametric multilayered plate finite element is employed. The von Kármán nonlinear theory is adopted in conjunction with the total Lagrangian formulation and the full Newton method. An extensive description of the finite element formulation used can be found in Ref. 8. An FEM mesh of two elements has achieved the convergent solution. The geometrical, material, and layup data are the same as that in Sec. II. A reduced integration technique has been used to avoid locking. Table 1 compares the analytical and FEM models. Both linear and nonlinear results are given. Several values of the applied load N_x^0 and two layups are considered. This table only considers the load control method, which fails to correspond to the two-layer plate loaded in compression by $N_x^0 = -3$ lb/in. There is very good agreement between the two models in the linear analysis. However, the nonlinear analysis shows that decreasing the number of the layers and increasing the modulus of N_x^0 greatly increases the disagreement. The results related to the in-plane tension loading case are plotted in Fig. 1. We note that as the N_x^0 values increase, the differences between the analytical and the FEM model increase considerably. Furthermore, this loading case, from only a qualitative point of view, shows the same behavior between the two models. In fact, the FEM analyses seem to present the asymptotes corresponding to values of W_c greater than $W_{\max}$. Increasing B_{11} increases the absolute values of the differences between the two models although their relative values are rather constant.

Very different behavior is shown by considering the in-plane compression loading case. In fact, Fig. 2 shows that even if a low level of the applied loads is considered, the predictions of the analytical model are completely wrong. The analytical model cannot go beyond the values $N_{\max}$. With L decreasing, i.e., with the coupling stiffnesses magnitude B_{11} increasing, the disagreement between the two models is increased greatly indeed. Furthermore, for the two-layer case, Fig. 2 shows a rather new result: a limit point can be found in the nonlinear response of asymmetrically laminated compressed plates. Because an unstable equilibrium path is possible, the snapping occurs. The failure of the control load methods quoted in Table 1 must be related to this phenomena (in such cases instead of the load control method, we have implemented an arc length type method, or Riks method, which consists of a modified version of that originally presented by Crisfield, and it has been extensively presented by the author in Ref. 8). The possibility of the snap through is directly related to the magnitude of coupling stiffnesses B_{11}. Because of the different order of magnitude of W_c, before and after the inflection (or the limit point), Fig. 3 considers, with the W_c axis in a simple logarithmic scale, the extension of the FEM results of Fig. 2 to larger displacements. This figure shows the existence of a limit point in correspondence with the 2-, 4-, and 10-layer cases, whereas the 20-layer case seems to present an inflection point. Naturally, these limit points are achieved at different values of the applied loads.

Concerning the different level of accuracy given by the analytical model between the plate in tension and compression, Figs. 1–3 confirm what was foreseen in the end of Sec. II. In fact, especially when a limit point exists, the nonlinear terms have a dramatic effect and cannot be neglected.

IV. One-Degree-of-Freedom Model

Through the use of a one-degree-of-freedom elastic model, this section explains in a very simple manner what has been obtained previously. The one-degree-of-freedom model given in the sketch of Fig. 4 comes from that presented by the author in Ref. 8 to explain the disappearance of the bifurcation point in unsymmetrically laminated composite plates subjected to axial compression. P, B, s, l, and α denote the applied load, coupling force, stiffness of the torsional spring, length of the rigid bar, and the chosen unknown, respectively; and u and w are the displacements along the P and B directions, respectively. Let us consider two different forms of the coupling force B.

First we consider the form $B = bP$. This is the original form quoted in Ref. 8. Here, b is a coupling coefficient. The equilibrium paths hold

$$\text{(I)}\quad \frac{Pl}{s} = \frac{\alpha}{\sin\alpha + b\cos\alpha}\,; \qquad \text{(II)}\quad \alpha = 0 \tag{9}$$

The path $\alpha = 0$ exists if and only if $b = 0$. The case $b = 0$ simulates the behavior of symmetrically laminated plates subjected to axial compression. In fact, the buckling of the bifurcation type occurs when $(P_{cr}l/s) = 1$. When $b \neq 0$, the model simulates the results from FEM analysis.

Looking for a simulation of the analytical model in Sec. II, let us consider the linearized solution of Eq. (9). We obtain $(Pl/s) = [\alpha/(\alpha + b)]$. This result perfectly simulates the disagreement between the analytical and the FEM analyses in Fig. 1. In fact, the linearized solution shows the asymptote at a linearized value $\alpha = -b$ instead of the exact value of $\alpha = -\arctan(b)$. The preceding model has not been able to simulate the limit-point cases found in the FEM models. To find such a situation we consider a more accurate form of the coupling phenomena by adding a coupling term directly related to the axial displacement u, i.e., by means of an additional coupling parameter h: $B = bP + hu$. Now the coupling is an effective internal stiffness. The equilibrium conditions become

$$\text{(I)}\quad \frac{Pl}{s} = \frac{\alpha - (hl^2/s)(\cos\alpha + 2\sin^2\alpha - 1)}{\sin\alpha + b\cos\alpha}\,;$$

$$\text{(II)}\quad \alpha = 0 \tag{10}$$

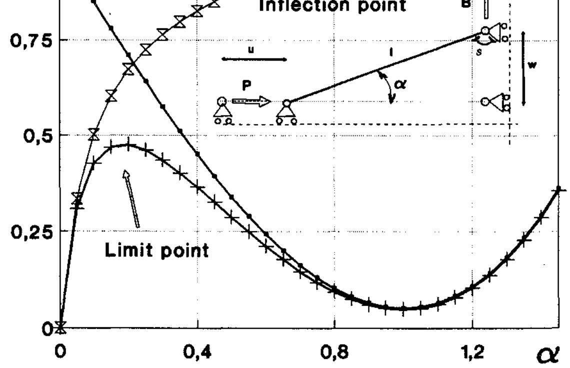

Fig. 4 One-degree-of-freedom model in compression, $B = bP + hu$ case, exact solution: load deflection curves for several values of the coupling parameters b and h.

Different equilibrium paths related to several values of the coupling parameters b and h are plotted in Fig. 4. At the value of $b = 0$, a bifurcation point exists corresponding to a new path start. When $b \neq 0$ the bifurcation point disappears and the equilibrium paths related to different values of the h parameter become asymptotic to that related to $b = 0$. For example, the path related to the $b = 0.1$, $h = 0.01$ values presents an inflection point, whereas for the $b = 0.1$, $h = 1$ value, the bifurcation point becomes a limit point and the snap through exists. By comparing Fig. 4 to Fig. 3 we can conclude that the present one-degree-of-freedom model perfectly simulates the behavior of long flat plates loaded in compression.

V. Concluding Remarks

Concerning the analysis of the nonlinear response of the cylindrical bending given by in-plane axial loads of asymmetrically laminated plates of cross-ply type, this Note has presented and compared results of three different models. The first model is an analytical one as proposed by Sun and Chin, the second consists of an FEM model, and the last one consists of a one-degree-of-freedom model. This study has confirmed that as the coupling stiffness magnitude increases, the importance of the nonlinear effects increases, and these effects cannot be neglected even when low levels of the applied load are considered. Furthermore, the following new conclusions can be noted. 1) The linearized nature of the Sun and Chin model has been shown, and its inadequacy to forecast the nonlinear response of the plates has been pointed out. 2) The FEM analysis has confirmed the preceding point, and a different level of accuracy of the analytical model between the tension and the compression loading cases, respectively, has been established. 3) The FEM analysis has shown the possibility of snapping in the nonlinear response of long plates in compression. In such a case the nonlinear effects could be dramatic. 4) The one-degree-of-freedom model has shown, in a simple manner, the conclusions given in the preceding points.

Additional investigations directed toward relating the snapping to some mixed geometrical stiffness parameter of the plate are needed. These studies should take into account different geometrical and mechanical boundary conditions. Furthermore, a mathematical treatment addressed to explain the failure of the analytical model would be welcome, which could be a subject for future work.

Acknowledgments

The author gratefully acknowledges Bernd Kröplin, director of the Institute of Static and Dynamic of the University of Stuttgart, for his helpful suggestions in developing the finite element method model vs the nonlinear and stability analyses. It is also a pleasure to thank Ettore Antona for his encouragements in the present study.

References

[1]Ambartsumyan, S. A., "Theory of Anisotropic Shells," NASA TTF-118, 1964.

[2]Stavsky, Y., and Reissner, E., "Bending and Stretching of Certain Types of Heterogeneous Aeolotropic Elastic Plates," *Journal of Applied Mechanics,* Vol. 28, 1961, pp. 402–408.

[3]Chia, C. Y., *Nonlinear Analysis of Plates,* McGraw-Hill, New York, 1980.

[4]Leissa, A. W., "Conditions for Laminated Plates to Remain Flat Under In-Plane Loading," *Composite Structures,* Vol. 6, 1986, pp. 261–270.

[5]Sun, C. T., and Chin, H., "Analysis of Asymmetric Composite Laminates," *AIAA Journal,* Vol. 26, No. 6, 1988, pp. 714–718.

[6]Sun, C. T., and Chin, H., "On Large Deflection Effects in Unsymmetric Cross-ply Composite Laminates," *Journal of Composite Materials,* Vol. 22, 1988, pp. 1045–1059.

[7]Barbero, E. J., and Reddy, J. N., "Nonlinear Analysis of Composite Laminates Using a Generalized Laminated Plate Theory," *AIAA Journal,* Vol. 28, No. 11, 1990, pp. 1987–1994.

[8]Carrera, E., "Postbuckling Behaviour of Multilayered Shells," Ph.D. Thesis, Dias, Politecnico di Torino, Torino, Italy, 1991.

[9]Palazotto, A. N., and Dennis, S. T., *Nonlinear Analysis of Shell Structures,* AIAA Education Series, AIAA, Washington, DC, 1992.

[10]Chen, H. P., and Shu, J. C., "Cylindrical Bending of Unsymmetric Composite Laminate," *AIAA Journal,* Vol. 30, No. 5, 1992, pp. 1438–1440.

[11]Carrera, E., "The Effects of Shear Deformation and Curvature on Buckling and Vibrations of Cross-Ply Laminated Composite Plates," *Journal of Sound and Vibration,* Vol. 150, 1991, pp. 405–433.

[12]Di Sciuva, M., and Carrera, E., "Static Buckling of Moderately Thick, Anisotropic Laminated and Sandwich Cylindrical Shell Panels," *AIAA Journal,* Vol. 28, No. 10, 1990, pp. 1782–1793.

Improved Method for Evaluating Damping Ratios of a Vibrating System

M. Liu*
Jilin University of Technology, Changchun 130022, People's Republic of China
and
D. G. Gorman†
Robert Gordon Institute of Technology, Schoolhill, Aberdeen AB9 1FR, Scotland, United Kingdom

Nomenclature

$[A]^\alpha$	= αth order spectrum factorization to matrix A
$[C]$	= damping matrix
$[\bar{C}]$	= modal transformed damping matrix
$\bar{C}_{\alpha\beta}$	= partitions of modal transformed damping matrix, $\alpha = k, d$, $\beta = k,d$
$[C_{cr}][D_{cr}]$	= critical damping matrices
$[D_{cr}]_k$	= truncated critical damping matrix associated with kept modes
$[I]$	= identity matrix
$[K]$	= stiffness matrix
$[M]$	= mass matrix
$[X]$	= general displacement vector
$[\Phi]$, $[\Psi]$	= right and left eigenvector matrices
$[\Phi_q]$, $[\Psi_q]$	= transformed right and left eigenvector matrices
$\Phi_k, \Phi_d, \Psi_k, \Psi_d$	= kept and deleted eigenvector matrices
Φ_r, Ψ_r	= residual right and left modes
$[\Lambda]$	= diagonal eigenvalue matrix
Λ_k, Λ_d	= kept and deleted eigenvalue matrices
$[\Lambda_r]$	= matrix obtained by residual mode transformation
α_i, β_i	= eigenvalues
λ	= scalar or eigenvalue
$[\xi]$	= Inman's criterion matrix
ζ_i, ξ_{ik}	= eigenvalues of $[D_{cr}]$ and $[D_{cr}]_k$

Introduction

IN the analysis of a dynamic system, inclusion of a damping matrix is almost unavoidable since it can often have a critical bearing on stability and dynamic responses. Damping ratios derived to classify modes of vibration determine the

Received Dec. 6, 1991; revision received Dec. 29, 1992; accepted for publication Jan. 5, 1993.

*Currently Associate, Petroleum Science and Technology Institute, Robert Gordon Institute of Technology, Schoolhill, Aberdeen AB9 1FR, Scotland, United Kingdom.

†Professor and Head, School of Mechanical and Offshore Engineering.